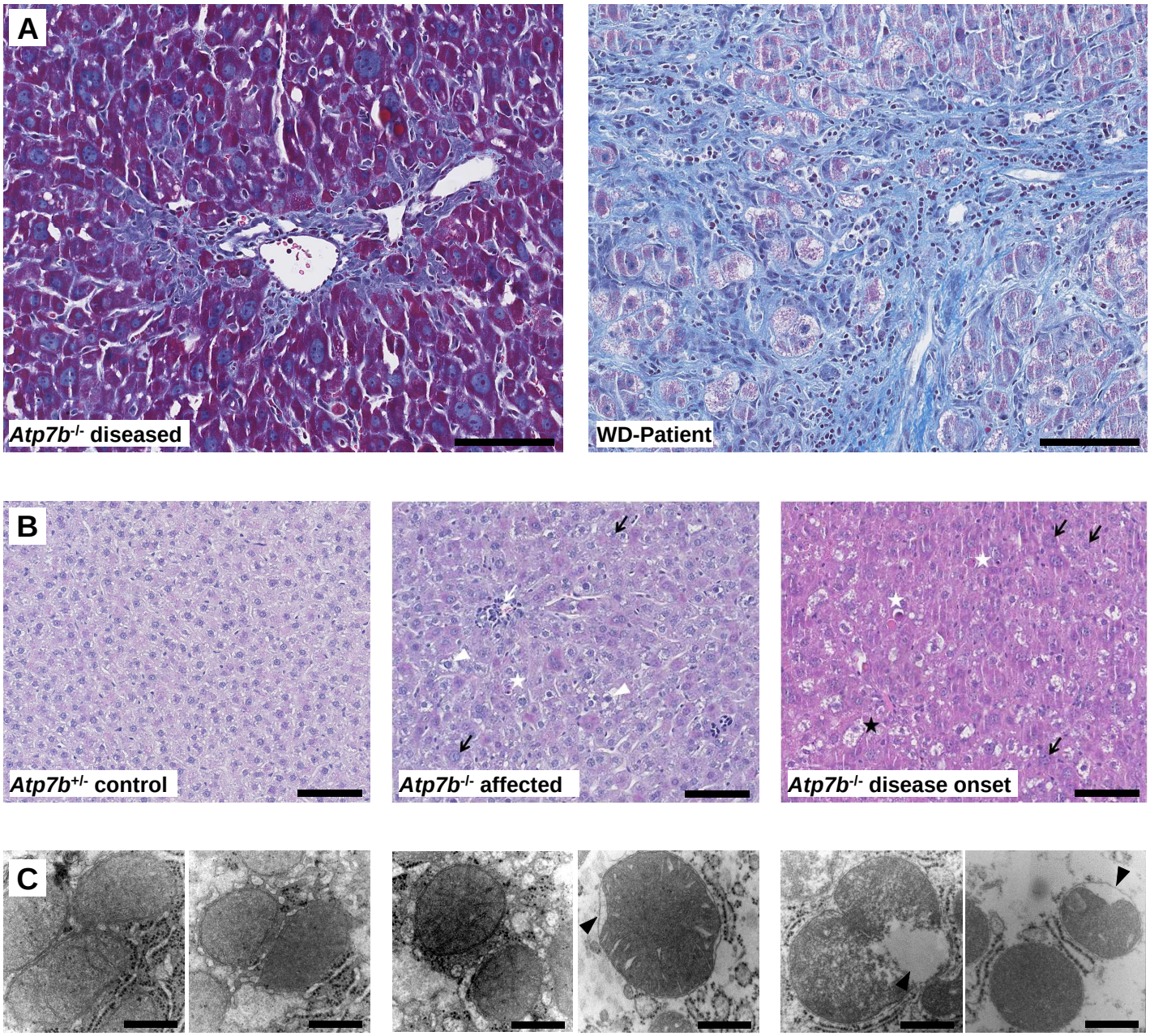

Supplementary Figure 1:

(**A**) Masson trichrome staining demonstrates signs of fibrosis (stained blue) in diseased *Atp7b*$^{-/-}$ rat liver (left panel) but marked fibrosis in an explanted untreated WD patient liver (right panel). Scale bar: 100 µm.

(**B**) H&E staining of *Atp7b* rat livers at different disease states shows increasing alterations during progression of the disease (Scale bar: 100 µm; white asterisk: different stages of apoptosis, black arrow: anisokaryosis, black asterisk: ballooned hepatocytes, white arrow: inflammatory infiltrates; white arrowhead: cytoplasmic condensation). One representative image is shown; *Atp7b*$^{+/-}$ control: n=16, *Atp7b*$^{-/-}$ affected: n=8, *Atp7b*$^{-/-}$ disease onset: n=6.

(**C**) Electron micrographs of *Atp7b* rat liver mitochondria in situ corresponding to the disease states as in B (Scale bar: 500 nm). Separated inner and outer membranes are indicated by arrowheads. Number of experiments as in (B).

Supplement Figure 2

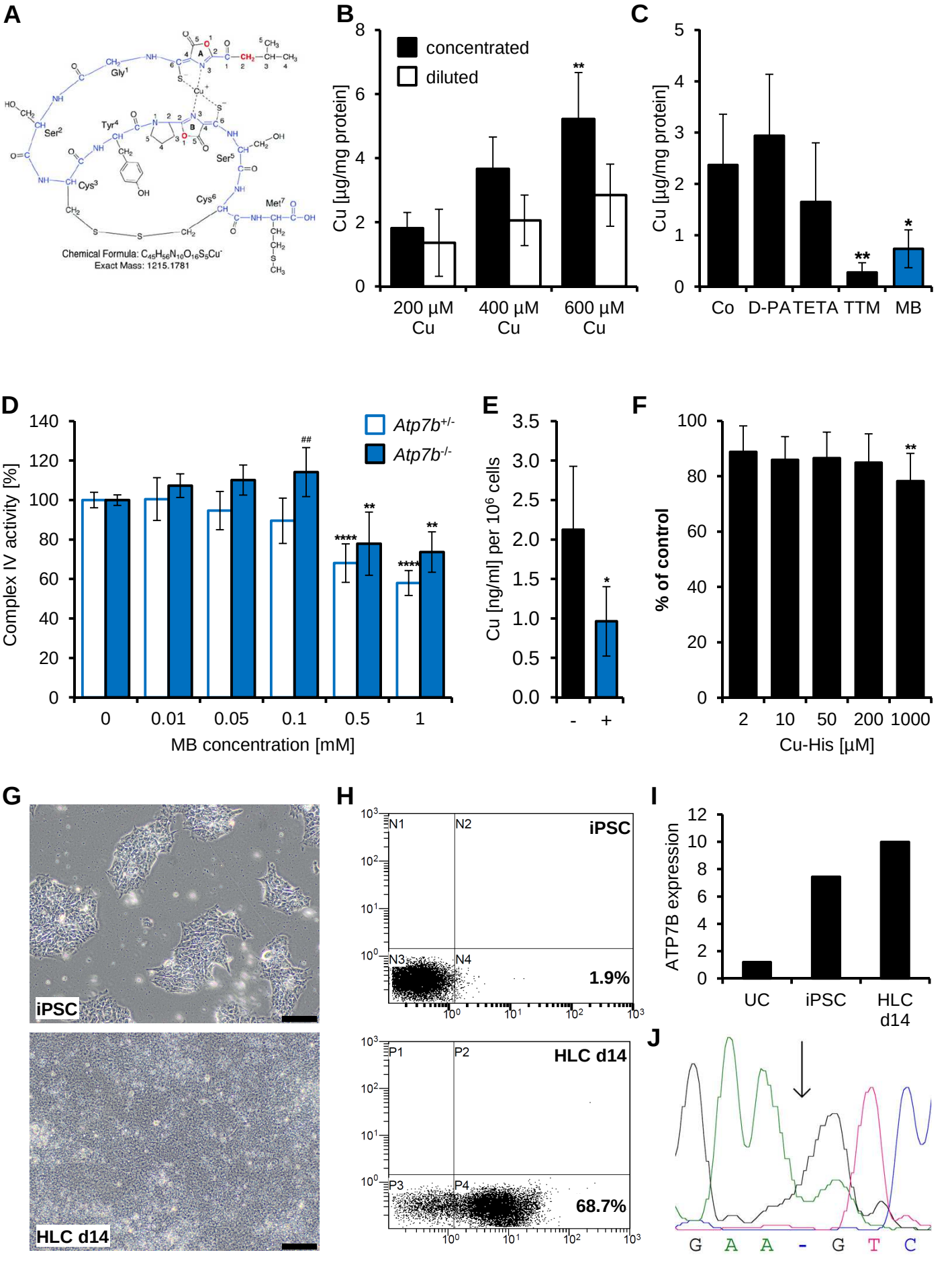

Lichtmannegger et al.

Supplementary Figure 2:

(**A**) Structural formula for Cu-methanobactin reproduced from (29): NMR, mass spectrometry and chemical evidence reveal a different chemical structure for Methanobactin that contains oxazolone rings. Lee A. Behling, Scott C. Hartsel, David E. Lewis, Alan A. DiSpirito, Dong W. Choi, Larry R. Masterson, Gianluigi Veglia, and Warren H. Gallagher. Journal of the American Chemical Society 2008 130 (38), 12604-12605. DOI: 10.1021/ja804747d with permission by ACS.

(**B**) Copper loading of isolated wildtype rat liver mitochondria. Mitochondria (4 mg/ml) were pre-incubated with DTT (1 mM), challenged with concentrated (20 mM) or diluted (2 mM) copper stock solutions, re-purified by density gradient centrifugation, and their copper load determined (N=4). *Significant to concentrated 200 µM Cu.

(**C**) Copper pre-loaded mitochondria from (B) were incubated with copper chelators (2 mM) for 30 min, and subsequently re-purified by density gradient centrifugation. (N=4-5; *significant to control).

(**D**) Comparison of the effect of MB to *Atp7b*$^{+/-}$ control mitochondria vs. *Atp7b*$^{-/-}$ mitochondria on copper-dependent mitochondrial respiratory complex IV activity (*Atp7b*$^{+/-}$: N=3, n=9, *Atp7b*$^{-/-}$: N=2, n=6; *significant to buffer control, $^{\#}$significant to respective concentration of *Atp7b*$^{+/-}$).

(**E**) MB treatment causes a 50% reduction of copper in HepG2 cells with basic copper load (N=3, (-) untreated control, (+) 24 h 500 µM MB treated, unpaired 2-tailed t-test with Welch's correction, *significant to untreated control).

(**F**) Dose dependent toxicity (neutral red) of histidine bound copper on HepG2 cells (N=5; *significant to culture medium control).

(**G- J**) Characterization of the WD patient derived HLCs from Figure 3C. HLCs at day 14 (but not iPSCs) present with (G) hepatocyte like morphology (Scale bar: 100 µm), (H) albumin marker and (I) pronounced *ATP7B* mRNA expression. (J) Sequence analysis of WD iPSC confirmed a homozygous deletion at position 2532 (c.2532delA, p.K844Kfs).

One-way ANOVA with Tukey's multiple comparisons test in B-D and F.

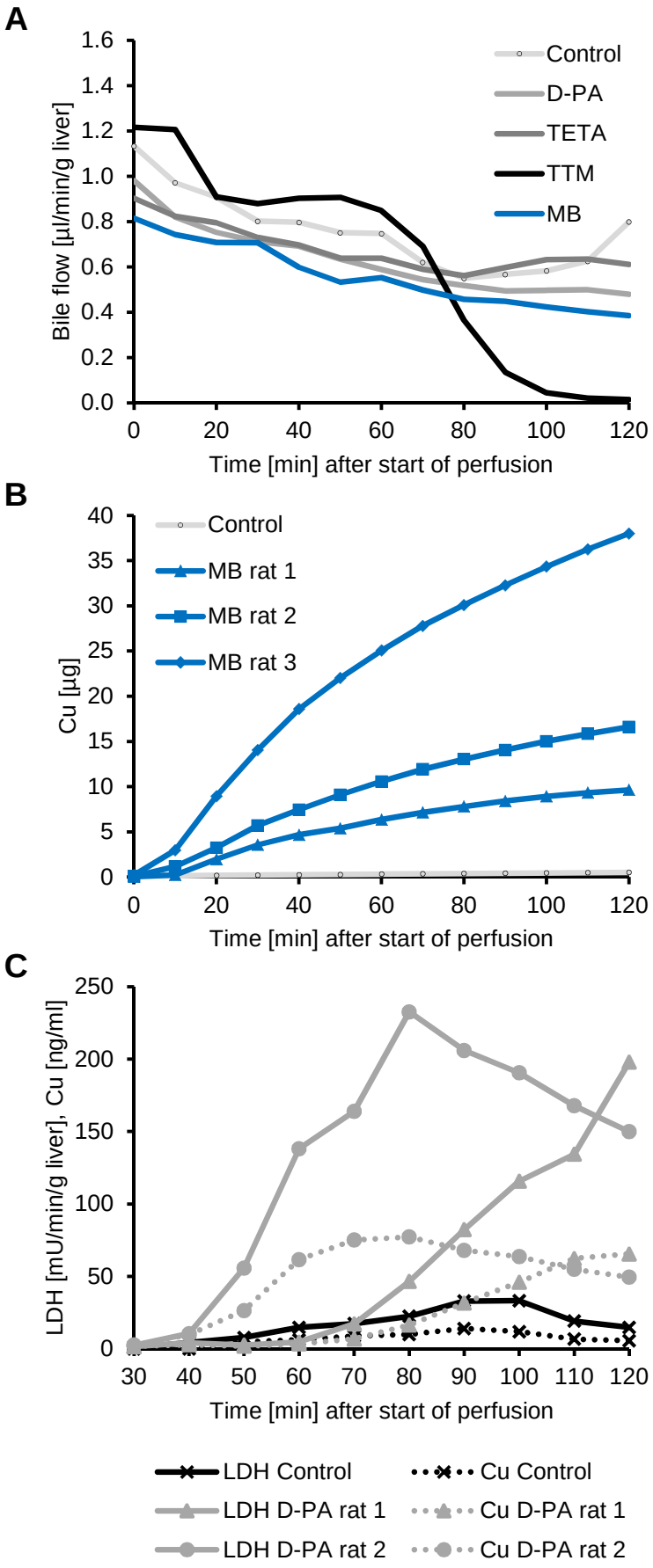

Supplementary Figure 3:
(A) Bile flow during two hour *Atp7b*$^{-/-}$ liver perfusion. Displayed are mean values of three independent experiments.
(B) Cumulative biliary copper excretion during two hour *Atp7b*$^{-/-}$ liver perfusion by MB (N=3).
(C) Parallel LDH and copper release into the perfusate during two hour *Atp7b*$^{-/-}$ liver perfusion.

Supplement Figure 4

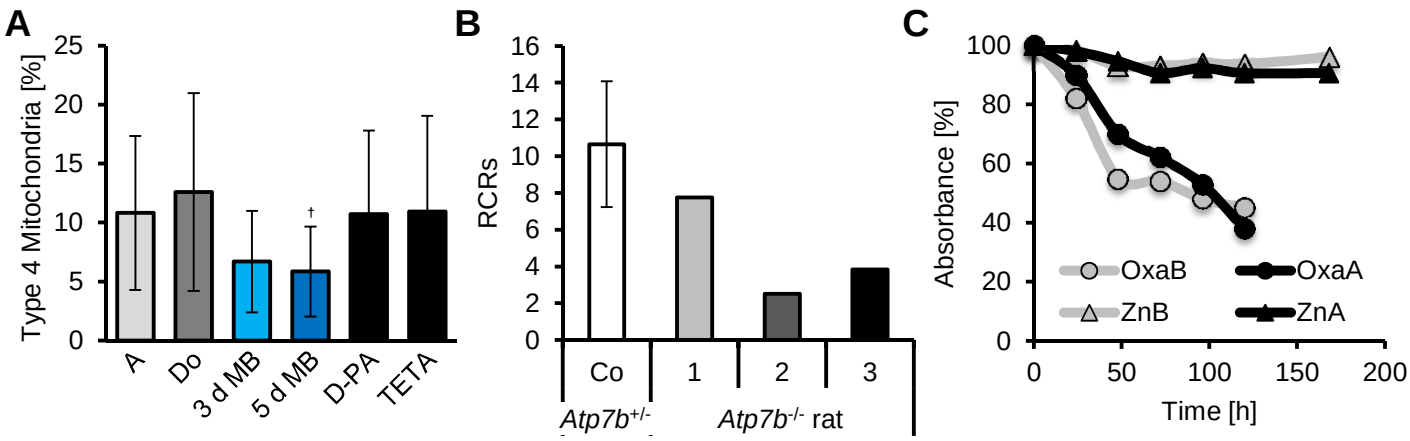

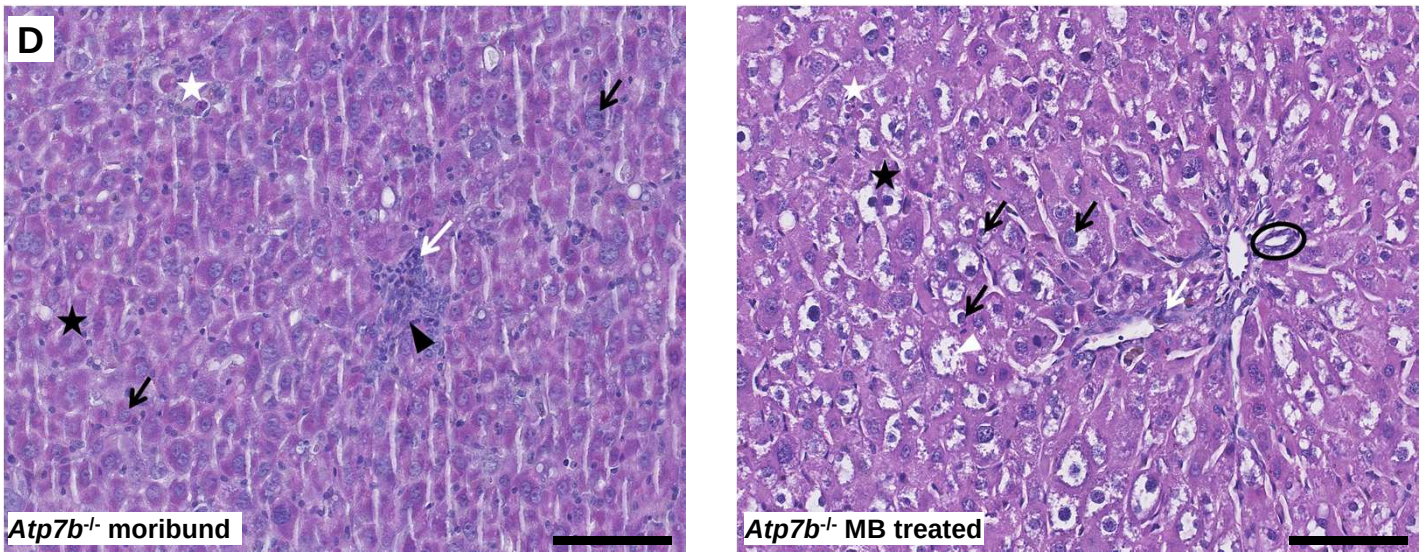

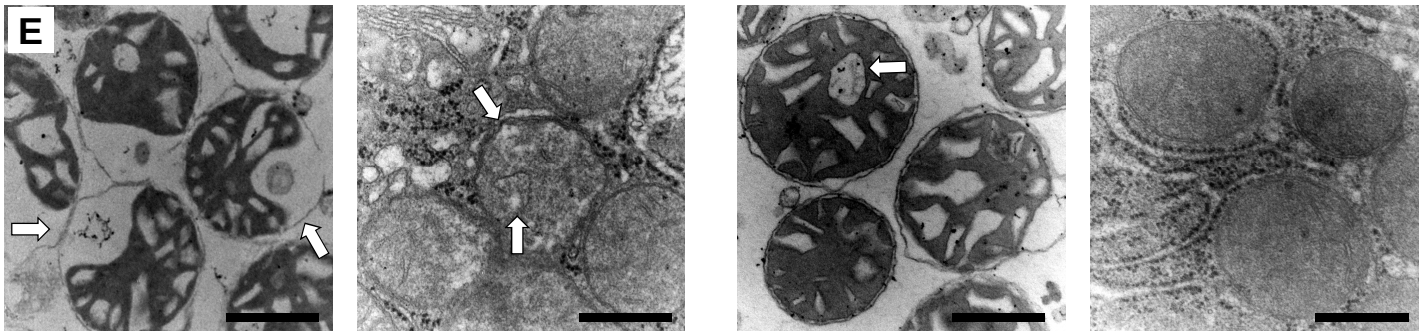

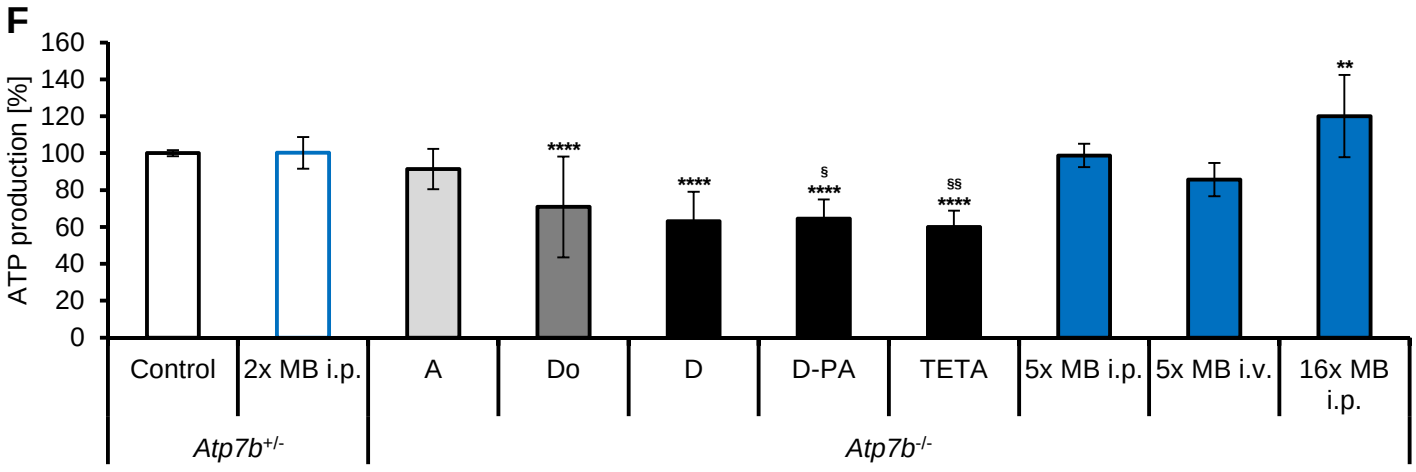

Lichtmannegger et al.

Supplementary Figure 4:

(**A**) Quantification to Figure 4D. Reduced numbers of severely impaired mitochondria (Type 4) were isolated from short-term MB-treated *Atp7b*$^{-/-}$ rats but not from untreated, D-PA- or TETA-treated *Atp7b*$^{-/-}$ animals, (N=number of EM micrographs, n=number of mitochondria; (A) Affected: N=31, n=807; (Do) Disease onset: N=24, n=734; 3 d MB: N=12, n=291; 5 d MB: N=18, n=460; D-PA: N=10, n=221; TETA: N=12, n=329). †Significant to disease onset.

(**B**) Respiratory analysis of mitochondria from MB-treated *Atp7b*$^{-/-}$ rats in Figure 5A-D. Mitochondria from the healthy animal (no. 1) were as intact as control mitochondria (respiratory control ratio with succinate as substrate, RCR_S, N=3), mitochondria from the two diseased animals (no. 2, 3) were impaired.

(**C**) Stability analysis of metal-free MB and Zn-loaded MB by absorbance change of their two metastable oxazolone rings (OxaA/ZnA at 394 nm and OxaB/ZnB at 340 nm) at 37°C. Zn-MB is time-stable at 37°C. N=3.

(**D**) H&E staining of untreated (left) and MB-treated (right) moribund *Atp7b*$^{-/-}$ rat livers with less severe liver damage in the MB-treated animal indicating liver regeneration (Scale bar: 100 µm, symbols as in Figures 1, S1).

(**E**) Isolated (left) or in situ (right) mitochondria from the animals in (D). Only minor structural alterations (arrows) were observed in the MB-treated *Atp7b*$^{-/-}$ rat (Scale bar: 500 nm).

(F) Progressively impaired ATP production of mitochondria isolated from *Atp7b*$^{-/-}$ rats at different disease states. Short-term MB treatments reversed this impairment whereas D-PA and TETA did not. Data are outlier corrected, n=number of measurements, Control: n=47, 2x MB i.p.: n=7, (A) Affected: n=20, (Do) Disease onset: n=14, (D) Diseased: n=8, D-PA: n=4, TETA: n=4, 5x MB i.p.: n=4, 5x MB i.v.: n=6, 16x MB i.p.: n=8. *Significant to control, §significant to 5 d MB i.p.

One-way ANOVA with Tukey's multiple comparisons test in A and F.

Supplementary Table 1

	Control (+/-)	Affected (-/-)	Disease onset (-/-)	Diseased (-/-)
N (n)	4 (8)	3 (6)	4 (8)	3 (6)
DPH:				
Control	256 ± 7	258 ± 5	257 ± 7	259 ± 11
Triton	198 ± 1	197 ±1[a]	193 ± 4	199 ± 7
TMA-DPH:				
Control	328 ± 6	338 ± 7*	339 ± 5**	344 ± 4***
Triton	389 ± 3	390 ± 6	392 ± 6	398 ± 6**

DPH, TMA-DPH: Values given in [mPol]. [a] N=3, n=5

Supplementary Table 1:

Fluorescence polarization demonstrates physical alterations in mitochondrial membrane properties at the protein-lipid interface (TMA-DPH) but not at the membrane inner lipid phase (DPH) in *Atp7b*$^{-/-}$ vs. control mitochondria. N=number of rats, n=number of measurements. Data are mean ± SD and outlier corrected. One-way ANOVA with Tukey's multiple comparisons test. *Significant to control.

Supplementary Table 2

	Control (+/-)	Affected (-/-)	Disease onset (-/-)	Diseased (-/-)
N (n)	3 (6)	2 (4)	2 (3)	3 (5)
Start [min]	71 ± 26	32 ± 3 *	23 ± 3 **	9 ± 4 ***
End [min]	113 ± 35	80 ± 4	66 ± 0	47 ± 11 **

Supplementary Table 2:

Calcium-induced (100 µM) MPT can be efficiently inhibited by Cys-A (5 µM). This blocking effect is severely impaired in mitochondria from diseased and disease onset *Atp7b*$^{-/-}$ rats. Data are mean ± SD and outlier corrected. One-way ANOVA with Tukey's multiple comparisons test. *Significant to control.

Supplementary Table 3

	Control (+/-)	Affected (-/-)	Disease onset (-/-)	Diseased (-/-)
N (n)	3 (6)	3 (6)	2 (3)	3 (6)
Start [min]	116 ± 26	94 ± 9	77 ± 1	49 ± 19 ****##
End [min]	171 ± 9	163 ± 15	138 ± 1 **#	124 ± 8 ****###

Supplementary Table 3:

Atp7b$^{-/-}$ mitochondria lose their membrane potential at earlier time points compared to control mitochondria. Data are mean ± SD and outlier corrected. One-way ANOVA with Tukey's multiple comparisons test. *Significant to control, #significant to affected.